NASA CR-72295

FIRST SUMMARY REPORT

STUDY OF ROLLING-CONTACT PHENOMENA IN MAGNESIUM OXIDE

by

K. F. Dufrane and W. A. Glaeser

prepared for

NATIONAL AERONAUTICS AND SPACE ADMINISTRATION

September 25, 1967

CONTRACT NAS 3-6263, TASK ORDER NO. 4

Technical Management
NASA Lewis Research Center
Cleveland, Ohio
D. P. Townsend, Project Manager
E. V. Zaretsky, Research Advisor

BATTELLE MEMORIAL INSTITUTE
Columbus Laboratories
505 King Avenue
Columbus, Ohio 43201

ABSTRACT

The phenomena associated with rolling contact deformation was studied using steel balls rolling on MgO single crystals. The depth of slip was found to be velocity dependent in the [100] rolling direction. Fatigue spalls similar to those found in actual bearings were produced after extended numbers of rolling cycles. Addition of lubricant to the surface changed the slip mode and caused premature spalling. Actual dislocation arrays in the deformed track regions were observed by thin film transmission electron microscopy.

TABLE OF CONTENTS

STUDY OF ROLLING-CONTACT PHENOMENA IN MAGNESIUM OXIDE

by

K. F. Dufrane and W. A. Glaeser

SUMMARY

Rolling-contact experiments were performed on the cube faces of optical-quality magnesium oxide (MgO) single crystals. The rolling element was a 0.25-inch (0.635 cm)-diameter hardened SAE 52100 steel ball rolled either in the [100] direction (parallel to the cube edge) or in the [110] direction (at 45 degrees to the cube edge). The depth of slip was found to depend on the rolling velocity; increases in velocity brought a decrease in depth of slip that was explained in terms of dislocation dynamics. Extended numbers of rolling-contact cycles were found to cause spalling in the ball track similar to fatigue spalls found in rolling-element bearings. It was found that the track showed an initial width increase, followed by a plateau and a second width increase at the high number of cycles where spalling occurred. Wear of the ball and track was insufficient to explain the width increases.

Addition of a lubricant to the rolling element-MgO interface caused a dramatic change in slip mode that led to spalling at 10^3 cycles as opposed to 10^5 cycles for dry contact. Apparently, the lubricant interacted with the MgO to promote slip on the $\{110\}_{90}$ slip planes. Thin films of the track region were prepared for examination by transmission electron microscopy. The dislocation density was very high in MgO specimens subjected to only 100 rolling cycles, and the change in slip mode on lubricated specimens was evident. No evidence of crack formation was seen in the limited number of thin films that were viewed.

INTRODUCTION

The need for predictably reliable life in rolling-element bearings and gears operating in advanced power systems has focused attention on the major mode of failure in rolling-element-bearing-surface fatigue. In the past, much attention has been paid to the effects of operating parameters on element fatigue life. Factors influencing rolling-element-bearing fatigue life have been isolated, and improvements in life and reliability have been made by their control. However, very little is known about the basic mechanisms involved in the rolling-element-bearing fatigue process. Without this knowledge, improvement in bearing and gear performance can only be attained by painfully slow experimental methods.

A study was initiated at Battelle several years ago to determine the effect of rolling-contact stress on dislocation generation and interaction.[1] Since the generation, motion, and interaction of dislocations determine mechanical behavior of solid materials, it was considered essential that the analysis of the basic rolling-element-bearing fatigue mechanisms begin with dislocation theory.

Single-crystal magnesium oxide (MgO) was used as a simple model bearing material. Compared with actual bearing steels, MgO provides the advantage of simple and well-established slip systems. Large optical-quality single crystals are available that allow the study of rolling-contact phenomena without the influence of grain boundaries, inclusions, or impurities. Etch-pit techniques are well-established that permit observation of slip patterns by simple light microscopy. Magnesium oxide also has sufficient strength to resist crushing or excessive deformation under rolling-contact stress. Thus, as a starting point for understanding the complex phenomena responsible for bearing fatigue failures, MgO provides an excellent model bearing material.

TECHNICAL APPROACH

Limited plastic deformation is assumed to be a prerequisite for rolling-element-bearing fatigue. Plastic deformation involves generation and motion of dislocations. Interaction of the moving dislocations results in work hardening and crack initiation. It is presumed that these fundamental concepts are involved in the process of rolling-element-bearing fatigue and that general dislocation theory should provide a powerful tool for the development of a deeper understanding of the contact-fatigue process.

There are some significant differences between rolling-contact stress conditions and general structural stress conditions that must be kept in mind when analyzing the interplay between dislocations and applied stress. For the general case of structural stress, a member is subjected to a more or less static stress field, and, as in the case of a beam under tensile load, the entire section is stressed. Dislocations in the part are acted on by the stress field and move until they reach the surface or are stopped by other dislocations or contaminants. In rolling contact, on the other hand, a very small zone in a body is acted on by a moving concentrated stress field. Therefore, instead of moving until stopped by some obstacle, the dislocations may move only briefly as they are acted upon by the stress field when it moves by. While in structural stress conditions large arrays of dislocations are moved simultaneously and many local effects are averaged out, in rolling contact, one might expect local effects and individual dislocation interactions to become significant because of the limited field and time of dislocation-stress interplay.

Owing to the complexity of the rolling-contact state of stress and the large number of possible dislocation configurations that might develop, direct observation of the effects of rolling contact on dislocation configurations has been considered the best method to quickly determine any unique behavior. The general approach is to roll a ball back and forth over the surface of a crystal and observe the resulting dislocation configurations. A material with a simple slip system that does not deviate from its known slip habit under any stress conditions is desirable for such a study. Magnesium oxide fills this requirement very well. Except for impact conditions, it has six easy glide planes and one glide direction in each plane. Its lattice structure and slip systems are shown in Figure 1. Magnesium oxide has the rock-salt structure, which consists of two interpenetrating fcc lattices, one made up of positive ions and the other of negative ions. The rock-salt crystal structure is shown in Figure 1. Because MgO is highly ionic, slip does not occur on the close-packed (100) cube planes, but instead on the (110) cube diagonals as shown in Figure 1. Slip on the cube planes would bring like-charged ions into close proximity; thus, a significant energy barrier would have to be overcome for slip of one lattice space.

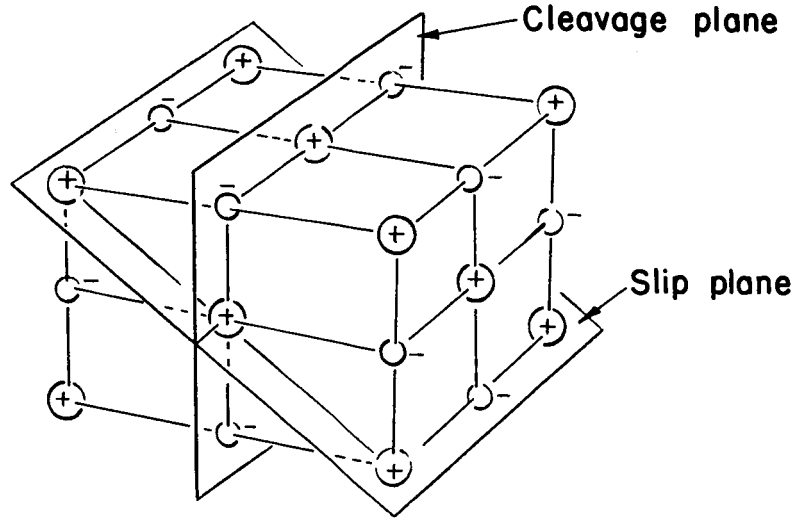

(a) Rock-salt structure

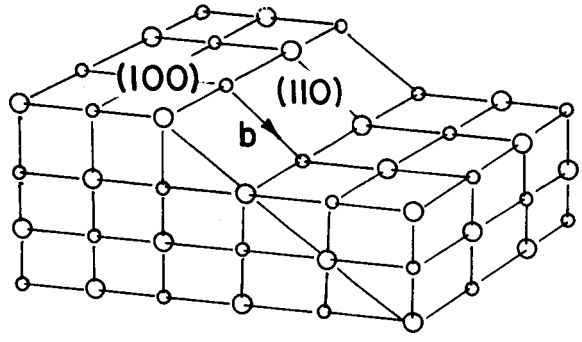

(b) MgO slip plane

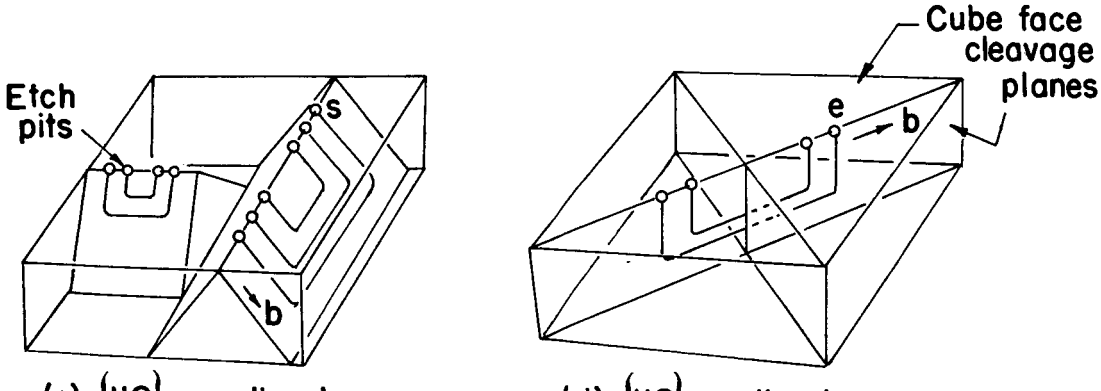

(c) $\{110\}_{45°}$ slip planes

(d) $\{110\}_{90°}$ slip planes

FIGURE 1. MAGNESIUM OXIDE CRYSTAL STRUCTURE, SLIP SYSTEMS, AND CLEAVAGE PLANES

Dislocation lines intersecting the crystal surface can be detected by treating the surface with a chemical etchant, which attacks the core of the dislocation and produces a pit. All rolling-contact experiments performed in this study were on the cleaved (001) cube faces of single-crystal MgO. Thus, the etch pits observed represent dislocation lines on the six easy slip planes shown in Figure 1(c) and (d). In Figure 1(c), two sets of (110) planes intersecting the cube face at 45 degrees are shown. These will be referred to as $\{110\}_{45}$ planes. The (110) planes that intersect the surface at 90 degrees are shown in Figure 1(d) and will be referred to as $\{110\}_{90}$ planes. It is assumed that plastic deformation occurs by operation of dislocation sources in which loops of dislocation lines move out over the slip planes under the action of a shear stress. When the loops intersect the cube face, the $\{110\}_{45}$ screw segments will be revealed by etching as shown in Figure 1(c). The $\{110\}_{90}$ loops will intersect edge segments as shown in Figure 1(d). The etch pits will tend to line up and delineate slip-plane intersections as straight lines on the (100) surface of the crystal. If all planes are operative, therefore, etch pitting will reveal lines intersecting at 45 degrees (two sets of mutually perpendicular lines). Crystallographic directions, as well as the slip planes, are shown in Figure 2.

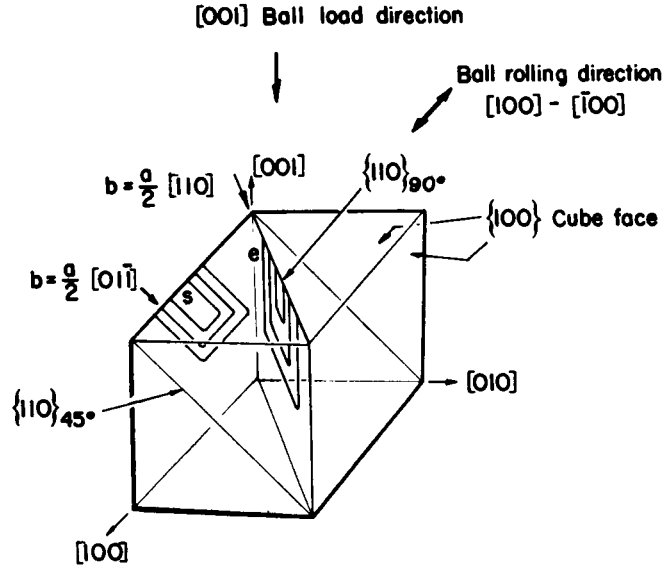

FIGURE 2. REFERENCE CUBE IN AN MgO SINGLE CRYSTAL

EXPERIMENTAL METHOD

Apparatus

The apparatus used for rolling a ball over a single crystal of MgO is shown in Figure 3. An 0.25-inch (0.635 cm)-diameter ball mounted on a shaft held between a conical pivot bearing is shown in contact with a rectangular crystal specimen. The ball mount is suspended under the triangular table, and the ball provides one point of a three-point contact configuration. The triangular table is driven by a crank-arm arrangement and

guided by two nylon feet that slide in a vee way. Deadweight loading is applied to the upper surface of the triangular table.

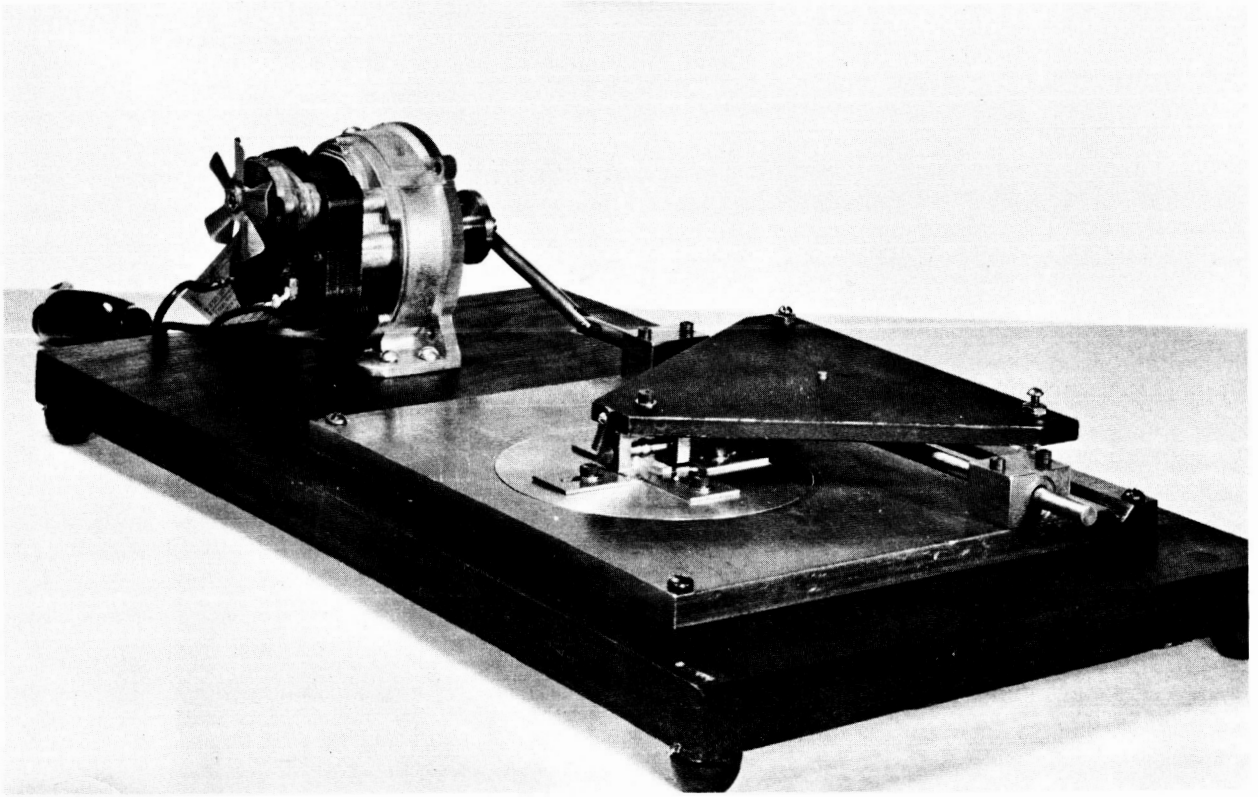

FIGURE 3. APPARATUS FOR APPLYING ROLLING-CONTACT STRESS

Operating Conditions and Procedure

With a cleaved and polished MgO single crystal mounted in the rolling-contact apparatus, the ball was rolled over the crystal surface under the following loads:

Ball Load		Calculated Maximum Hertzian Shear Stress			
		Steel		Stellite 3	
Pounds	Grams	1000 Psi	Kg/Mm^2	1000 Psi	Kg/Mm^2
0.54	244	40	28	45	32
0.84	378	46	33	48	34
1.26	570	53	38	60	42

The ball was moved back and forth over the same track on the crystal for the desired number of stress cycles. Maximum ball velocity was 1.6 inches/sec (4.07 cm/sec). The crystal was oriented so that the ball always rolled on the (001) surface and in either of two directions: [100]-[$\bar{1}$00] and [110]-[$\bar{1}$10]. Figure 2 shows the Miller indices as an aid in orienting ball rolling directions with respect to slip planes in MgO single crystals.

After subjecting a crystal to rolling-contact stress, it was removed from the apparatus and cleaved to cut the ball path at right angles or at 45 degrees (depending on the

crystallographic direction of the ball path. Magnesium oxide cleaves easily only on the cube planes (100), and therefore could not be cleaved at right angles to the [110] direction ball paths. The sections were then etched to reveal dislocations terminating at the surfaces. Dislocation etch pits were observed with a metallographic microscope at magnifications ranging from 200X to 500X.

Crystal Preparation

Optical-quality MgO single crystals were purchased from the Norton Company for use in the study. To minimize the dislocation density and facilitate cleaving, the bulk crystals measuring 3/4 x 3/4 x 1/4 inch (1.9 x 1.9 x 0.6 cm) were annealed in air at 1200 C for 24 hours and furnace cooled. A magnesite (industrial MgO) crucible was used as the container to avoid contamination. After annealing, the crystals remained completely colorless.

The bulk crystals were cleaved to a specimen size of approximately 1/16 x 1/4 x 3/4 inch (0.16 x 0.6 x 1.9 cm) using a chisel and hammer or a pendulum cleaver constructed following Gilman, et al.[2]. Production of flat surfaces was quite good, with a minimum of cleavage steps. To level the remaining surface, the crystals were chemically polished in orthophosphoric acid at 220 F for 1-minute intervals up to 5 minutes. The surface was inspected under a microscope at 50X after each minute to follow the leveling process. If cleavage steps or imperfections remained after 5 minutes of polishing, the crystal was discarded. This procedure produced very flat surfaces.

Materials Properties

The properties of the MgO crystal and the ball materials are tabulated below.

Material	Young's Modulus 10^6 Psi	Young's Modulus 10^4 Kg/Mm^2	Poisson's Ratio	Tensile Yield Strength 1000 Psi	Tensile Yield Strength Kg/Mm^2	Hardness
MgO	38	2.7	0.25	8 to 9	5.6 to 6.3	370 Knoop
AISI 52100 steel	29	2.0	0.3	200	140	62 R_C
Stellite 3	33	2.3	--	~80	56	60 R_C

Rolling-Contact Slip Characteristics

The preferred slip systems for various ball rolling directions are shown in diagram form in Figure 4. Etch-pit patterns expected from intersection of these slip systems with cleavage surfaces also are diagramed. The actual dislocation etch-pit patterns of a typical surface track and cross section after one rolling pass in the [100] direction are shown in Figure 5 and can be compared with the expected patterns in Figure 4. The [100] ball rolling direction produces slip lines both parallel and normal to the rolling direction resulting from slip on $\{110\}_{45}$ planes. In the cross section, the $\{110\}_{45}$ planes that intersect the surface parallel to the rolling direction cross beneath the surface. Previous work[1] has shown the crossing point to be very near the location of the maximum Hertzian shear stress and that it is probably the origin of the dislocations appearing on the slip planes. In section, the slip planes can be seen as two intersecting groups of slip planes.

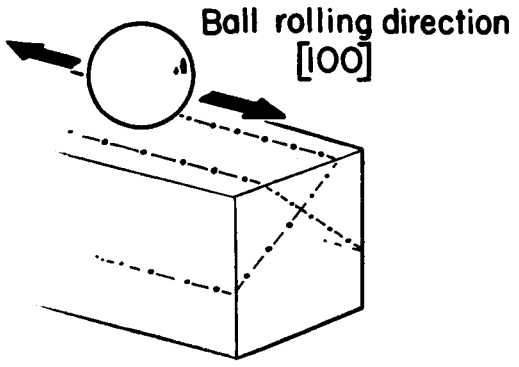

(a) (101) and ($\bar{1}$01) slip planes

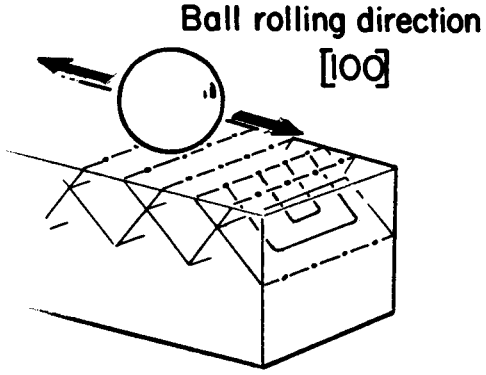

(b) (011) and (0$\bar{1}$1) slip planes

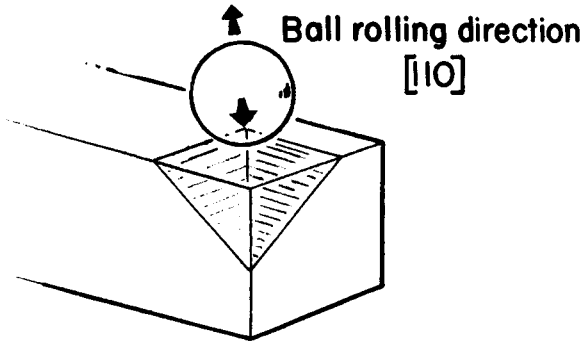

(c) (101) and (011) planes intersecting at 120° in front of ball rolling in [1$\bar{1}$0] direction

FIGURE 4. PREFERRED SLIP SYSTEMS IN SINGLE-CRYSTAL MgO FOR VARIOUS BALL ROLLING DIRECTIONS

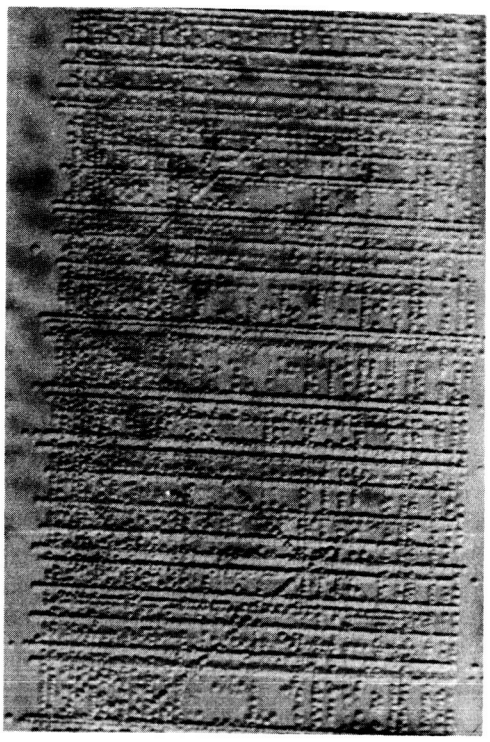

[100] rolling direction

500X

(a) Surface

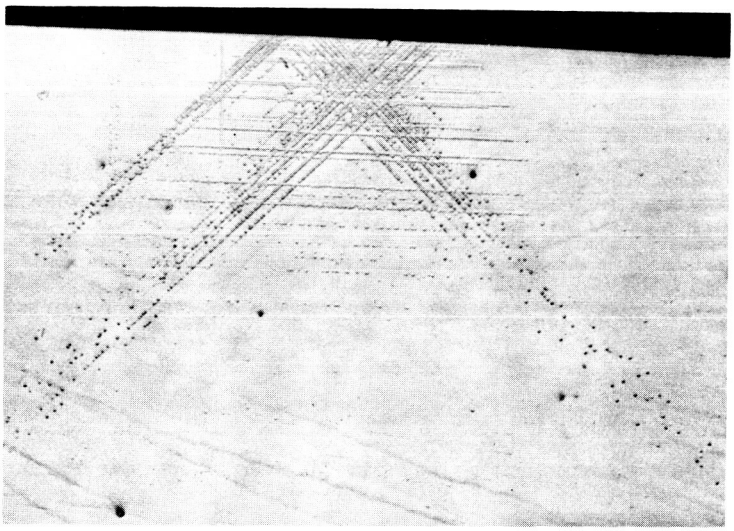

200X

(b) Cross section

FIGURE 5. DISLOCATION ETCH-PIT PATTERNS AFTER ONE ROLLING-CONTACT PASS AT A 570-GRAM LOAD

The depth of slip on the $\{110\}_{45}$ planes that intersect the surface parallel to the rolling direction is always greater than on the $\{110\}_{45}$ planes that intersect the surface normal to the rolling direction. This is seen in the cross section in Figure 5. The depth of penetration of the dislocations lying in a line at 45 degrees to the surface is greater than the depth of penetration of dislocations lying in a line parallel to the surface. This is probably the result of a dynamic interaction of the moving stress field with the propagating dislocations. Dislocations lying on the $\{110\}_{45}$ planes intersecting the surface parallel to the rolling direction are influenced by the shear stresses in the stress field for a longer time, since it is moving along the plane. Dislocations lying on the $\{110\}_{45}$ planes that intersect the surface normal to the rolling direction are not subjected to the stress field so long, since it moves continually away from the given plane, resulting in a lesser depth of penetration.

The following postulates have been made for the effect of rolling-contact stress on dislocation propagation in single-crystal MgO and their manifestation looked for in the experimental results:

(1) Since the dynamics of interacting moving stress fields and dislocations has been shown to be important, one would expect that, when the relative velocities of the stress field and dislocations are changed, the resulting distribution of dislocations should change.

(2) The anisotropy of dislocation propagation under rolling-contact stress should be significant in the interaction of intersecting dislocation loops. Dislocations intersecting on (101) and (011) planes (120-degree intersection) will interact to produce new dislocations on a (112) plane, an immobile plane in MgO. Continued operation of this interaction could be one way of work hardening prior to fatigue damage. Therefore, one might expect that dislocation density and the onset of spalling could be influenced by rolling direction.

(3) Slip systems resulting from rolling-contact stress on (100) surfaces are predominantly $\{110\}_{45}$. The dislocations on these slip planes intersect the surface as screw components. It is expected that cross slip of the surface screw components is required to multiply dislocations and increase the plastic strain. Changes in the surface state might be expected to alter the distribution of plastic strain.

EXPERIMENTAL RESULTS

Rolling-Velocity Effects

A series of experiments were performed to determine the effect of ball rolling velocity (translational velocity) on the nature of subsurface deformation. It was suspected that, if the ball rolling velocity exceeded the velocity of dislocations propagating from the region of maximum shear stress, the extent of subsurface deformation would be changed.

Experimental Method

A 0.25-inch (0.635 cm)-diameter hardened steel ball was rolled at a series of velocities at two different load levels in the [100] rolling direction. The following operating conditions were used:

Ball Load		Maximum Hertzian Shear Stress		Maximum Rolling Velocities	
Pounds	Grams	1000 Psi	Kg/Mm^2	In./Sec	Cm/Sec
0.54	244	40	28	2.5	6.35
1.26	570	53	38	3.76×10^{-1}	9.53×10^{-1}
				6.27×10^{-3}	1.59×10^{-2}
				1.14×10^{-4}	2.90×10^{-4}
				4.33×10^{-6}	1.10×10^{-5}

Since the motion of the ball across the specimen was produced by a crank arrangement, the velocity varied sinusoidally along the track. Therefore, in observing the effect of rolling velocity on subsurface dislocation configurations, only the central one-third of the MgO specimen was used. Within this portion of the specimen, rolling velocities varied from maximum to 85 percent of the maximum value. During this series, each experiment consisted of one rolling pass in the [100] direction over a fresh surface.

After each experiment, the crystal was cleaved four times in the central one-third portion normal to the rolling direction. The sections were etched to produce surface and subsurface etch pits. Measurements of track width and depth of slip on the $\{110\}_{45}$ planes that intersect the surface parallel to the rolling direction were made with a filar eyepiece at 200X. Duplicate specimens, each with three separate passes, were run for each load and rolling velocity, giving up to 40 measurements of depth for each combination.

Results and Discussion

The measurements of depth of slip from the surface on $\{110\}_{45}$ planes (measured along these planes) showed a definite decrease in depth with increasing ball rolling velocities. The relationship is plotted in Figure 6, with the standard deviation or the mean depth shown as a horizontal line through points on the curves. The depth of slip remained nearly constant at lower rolling velocities up to 10^{-2} cm/sec (0.004 in./sec). At higher velocities the depth of slip decreased. Both contact-stress levels showed a similar effect. Measurements of the track width at the surface showed no change with variations in rolling velocity.

The subsurface configuration of dislocation loops lying on $\{110\}_{45}$ planes that intersect the surface normal to the rolling direction was determined by measuring the width of the extremity of the loops as successive layers were removed from the surface by chemical polishing. Polishing was done in phosphoric acid at 220 F for 1-minute intervals, followed by etching to reveal dislocation etch pits. Dislocations on individual slip planes

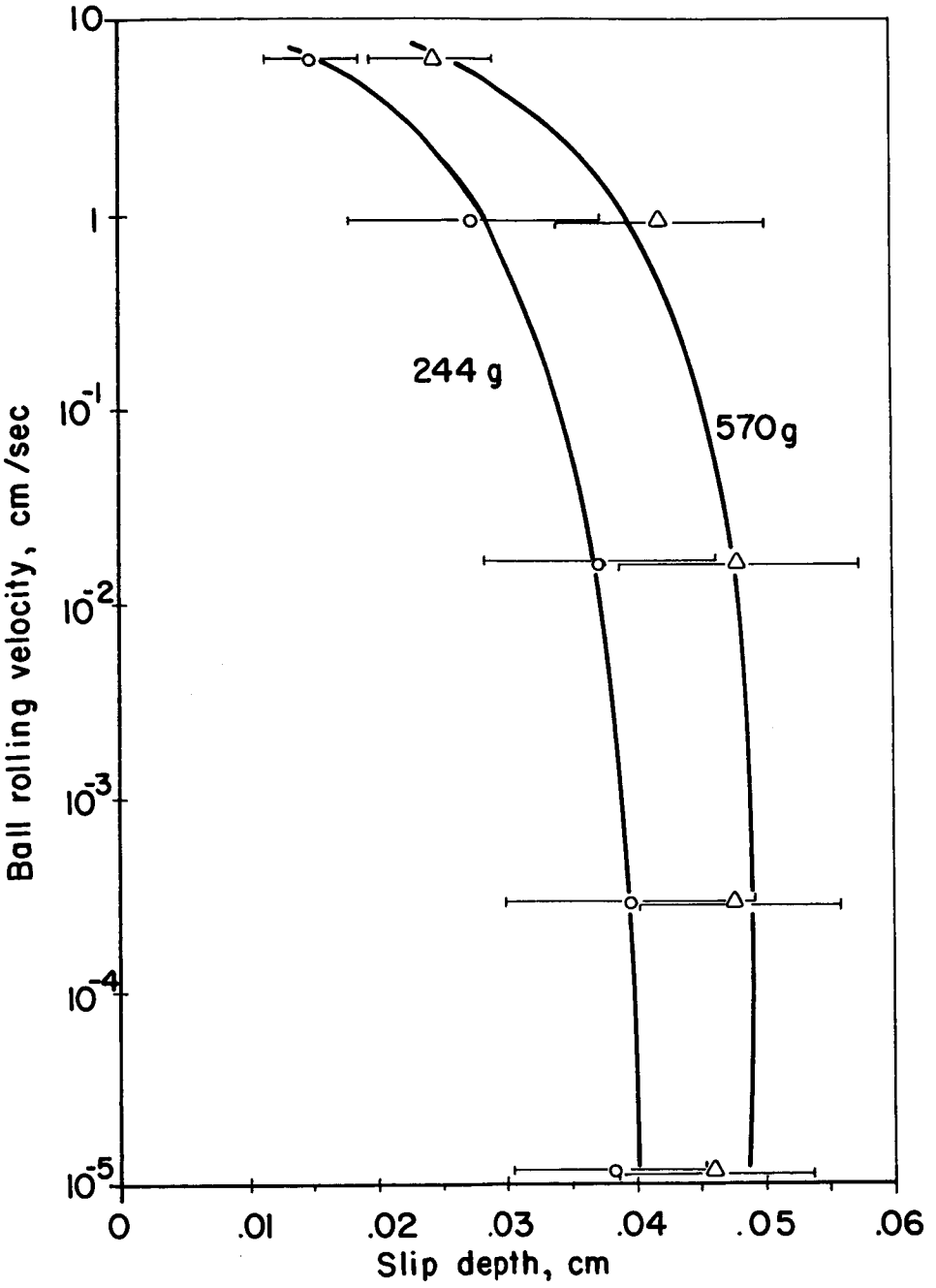

FIGURE 6. VARIATION OF SLIP DEPTH WITH ROLLING VELOCITY AT 244- AND 570-GRAM LOADS

were followed into the crystal by careful mapping of the segment of the track at each level to locate the slip line of interest in relation to adjacent lines.

The results of the width measurements at two rolling velocities are shown in Figure 7. Figure 7(a) shows the position of the loops on the (101) plane. Since the number of loops in the slip plane was very high, individual etch pits that formed where the loops intersected the surface were unresolvable, and only the extremities were measured. Representative dislocation-penetration analyses are shown in Figure 7, (b) and (c). The shape of the envelopes was similar and the width at the surface nearly identical. The extent of slip beneath the surface was velocity dependent, however, in the same manner as the depth of slip on the $\{110\}45$ planes parallel to the rolling direction. The subsurface widening of the loops probably resulted from the subsurface location of the maximum shear stress.

The decrease in depth of dislocation penetration with increasing rolling velocity is expected from a qualitative consideration of the effect of shear-stress level on dislocation velocity. Measurements by Johnston[3] show dislocation velocity increases in proportion to shear stress raised to the twenty-third power. Since the magnitude of the stress field induced by the contacting ball decreases rapidly away from the maximum stress region, the velocity of dislocations moving away from the high-shear-stress region into the crystal decreases rapidly. Therefore, as the ball's rolling velocities increase, sufficient time is not available for dislocations to move into the crystal.

Quantitative description of the effect is hindered by the interaction of the complex and varying stress field with the highly stress-dependent dislocation velocity. Accurate calculation of the Hertzian stress field is complicated by a violation of the basic criteria that all deformation be elastic and recoverable. Knowledge of the path of dislocation movement would also be required. Furthermore, the stress dependence of dislocation velocity reported by Johnston may not be applicable, because it was measured for half loops moving in a relatively dislocation-free crystal, a condition that does not exist in the rolling-contact experiments. These factors combine to make a quantitative analysis very difficult.

The absence of a dependence of track width on rolling velocity can be understood by considering the origin of the dislocations. As previously described, there is strong evidence that the dislocations originate in the vicinity of the maximum Hertzian shear stress. Since the distance to the surface is small and the stresses and corresponding velocities are high, the dislocations have ample time to reach the surface. Changes in track width would therefore require a change in the number of active slip planes, an effect more related to stress level than to rolling velocity.

The velocity effects described above may have some significance in actual rolling-contact situations. If the dispersal of dislocations becomes limited as rolling velocity is increased for a given stress state, one would expect a greater concentration of dislocations around their sources. It also is likely that multiplication of dislocations by cross slip of screw components to new slip planes would be reduced. The total result would be to concentrate plastic deformation around the maximum shear-stress zone and on a limited number of slip planes. Assuming this to be the case for multiple passes of the ball, fatigue damage would tend to appear on slip planes with high densities of dislocations. Dislocation interactions at intersecting planes or at inclusions and grain boundaries would be minimized because of the limited spread of deformation from the sources of dislocations. Propagation of fatigue cracks is promoted by precrack structural damage in zones where tensile stresses can operate on the crack front. Theories for crack initiation

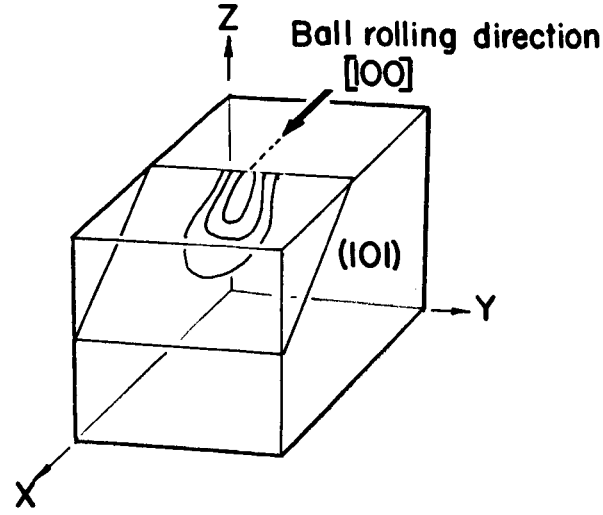

(a) Dislocation-loop location

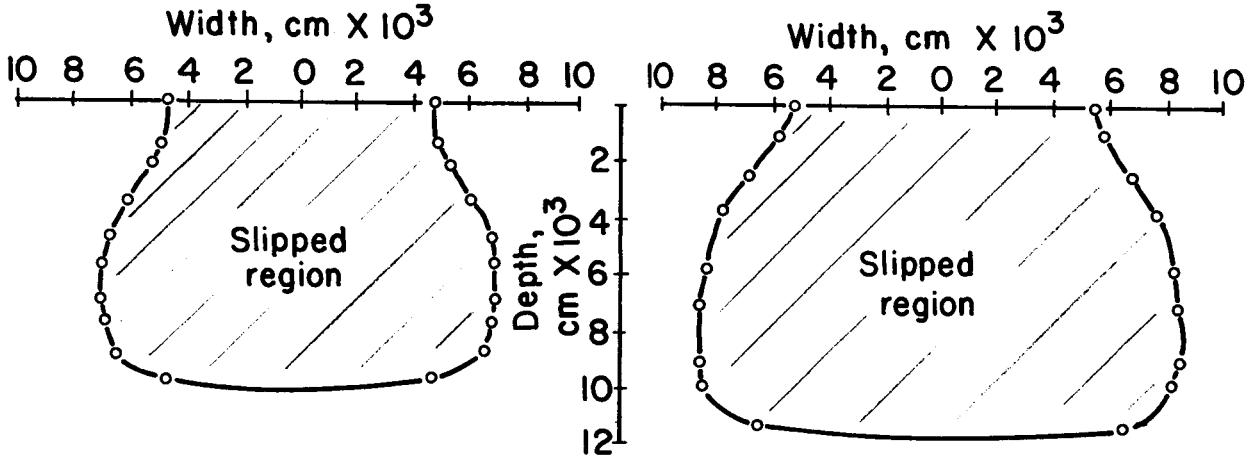

(b) 244 g, 635 cm/sec rolling velocity

(c) 244 g, 1.10 X 10^{-5} cm/sec rolling velocity

FIGURE 7. BOUNDARIES OF SUBSURFACE DISLOCATION LOOP CONFIGURATIONS

require pile-up of dislocations against obstacles such as grain boundaries, sessile dislocations, and inclusions. Concentration of dislocation distribution by velocity effects, then, might reduce the chances of interactions and reduce the field of damage caused by interaction. Therefore, it might be expected that a change in the mode of fatigue and possibly an increase in life would occur. The dislocation velocities are more sensitive to stress state in metals than in ionic solids. Therefore, critical rolling velocities would probably be greater than those observed for MgO. The effect of rolling velocity on bearing fatigue might be most noticeable in high-speed, lightly loaded bearings. Since grain boundaries are effective barriers to dislocations, the velocity effect may be expected to diminish with decreasing grain size in polycrystalline material.

The combined factors of rolling-contact velocity and maximum shear stress should be considered as significant factors in rolling-element-bearing deformation processes. The stress-velocity relationship for moving dislocations in bearing materials could be an important factor to consider for rolling-element bearings.

Accumulation of Deformation and Fatigue Spalling

Previous rolling-contact experiments with MgO indicated that dislocation density increases as the number of rolling cycles increases and that (110) slip planes that intersect at 120 degrees were favored during rolling in the [110] directions, as shown in Figure 4(c). Since sessile dislocations can form at these intersections, it was expected that dislocation accumulation and subsequent subsurface damage modes might be different, depending on the orientation of ball rolling direction.

Experimental Method

The effect of orientation was investigated in the following experiments in which the ball was rolled over MgO crystals in the [110] direction (45 degrees to the cube edge) for up to 10^6 cycles, and the track widths and damage were compared with similar experiments performed in the [100] direction.

All specimens were taken from the same MgO crystal to ensure consistency in defect concentration and hardness for comparison runs. A crystal measuring 3/4 x 3/4 x 1/4 inch (1.9 x 1.9 x 0.6 cm) was cleaved into three crystals measuring 3/4 x 3/4 x 5/64 inch (1.9 x 1.9 x 0.2 cm). Up to eight tracks were made in the [110] direction on each crystal under the following operating conditions:

Ball Load		Maximum Hertzian Shear Stress		Maximum Rolling Velocity		Duration,
Pounds	Grams	1000 Psi	Kg/Mm^2	In./Sec	Cm/Sec	cycles
0.54	244	40.3	28	2.5	9.53×10^{-1}	1
0.84	378	46.8	33			10
1.26	570	53.6	38			10^2
						10^3
						10^4
						10^5
						10^6

After tracks were produced on each specimen, it was cleaved into six pieces, etched, and examined. Track widths were measured with a filar eyepiece, and depths were measured with an interference microscope.

Results and Discussion

Figure 8 shows the variation in the width of the contact track with increasing numbers of cycles for three applied loads. Tracks from all three loads exhibited an initial width increase, followed by a plateau and a second increase after 10^4 cycles. Spalling in the tracks with the two heavier loads was observed after 10^5 cycles. Spalling was observed after 10^6 cycles with the 244-gram (0.54-pound) load. The results of rolling the ball in the [110] direction were compared with those of rolling the ball in the [100] direction at the same loads and rolling speed.[1] Track-width measurements from those experiments, shown in Figure 9, exhibit characteristics similar to those found when the ball was rolled in the [110] direction: an initial width increase, a plateau with track width remaining essentially constant, and a final increase in track width after approximately 10^4 cycles. Spalling occurred after 10^5 cycles, much in the same way as it did when the ball was rolled in the [110] direction. It appeared that the tracks in the [110] direction were somewhat wider than the tracks in the [100] direction for the same number of cycles at the lower cycle levels, but widened more rapidly to greater widths after 10^4 cycles. These variations were probably not significant, since the general shapes were similar and spalling occurred after approximately the same number of cycles. Some differences in dislocation distributions were observed, however, and these observations are discussed later.

The most interesting aspect of track-width characteristics is the second rise in track width and the associated spalling of the surface. Since wear of the unlubricated ball or track would cause an increase in measured track width at the larger number of cycles, experiments were performed to determine the extent of the wear and its possible influence on the widths.

A series of Talysurf measurements were made on a new hardened 52100 steel ball at intervals from 1 to 10^6 rolling cycles on MgO. These measurements showed that, although ball wear occurred, it was less than half the track width at any cycle level. Track widening, therefore, occurred well outside the actual ball-contact region. To minimize ball wear, a series of tracks with a 570-gram (1.26-pound) ball load were made with a

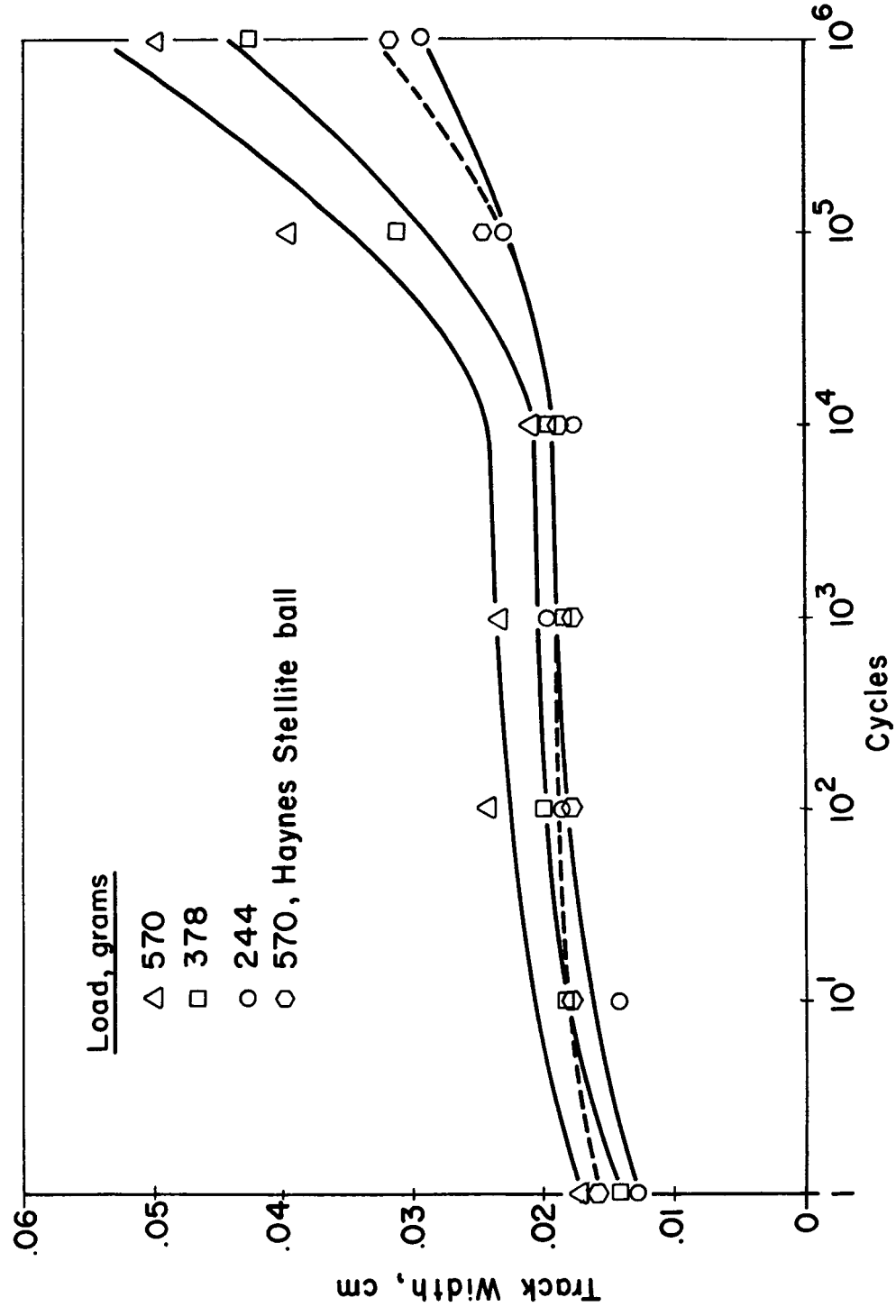

FIGURE 8. VARIATION OF TRACK WIDTH WITH NUMBER OF CYCLES FOR THE [110] BALL ROLLING DIRECTION

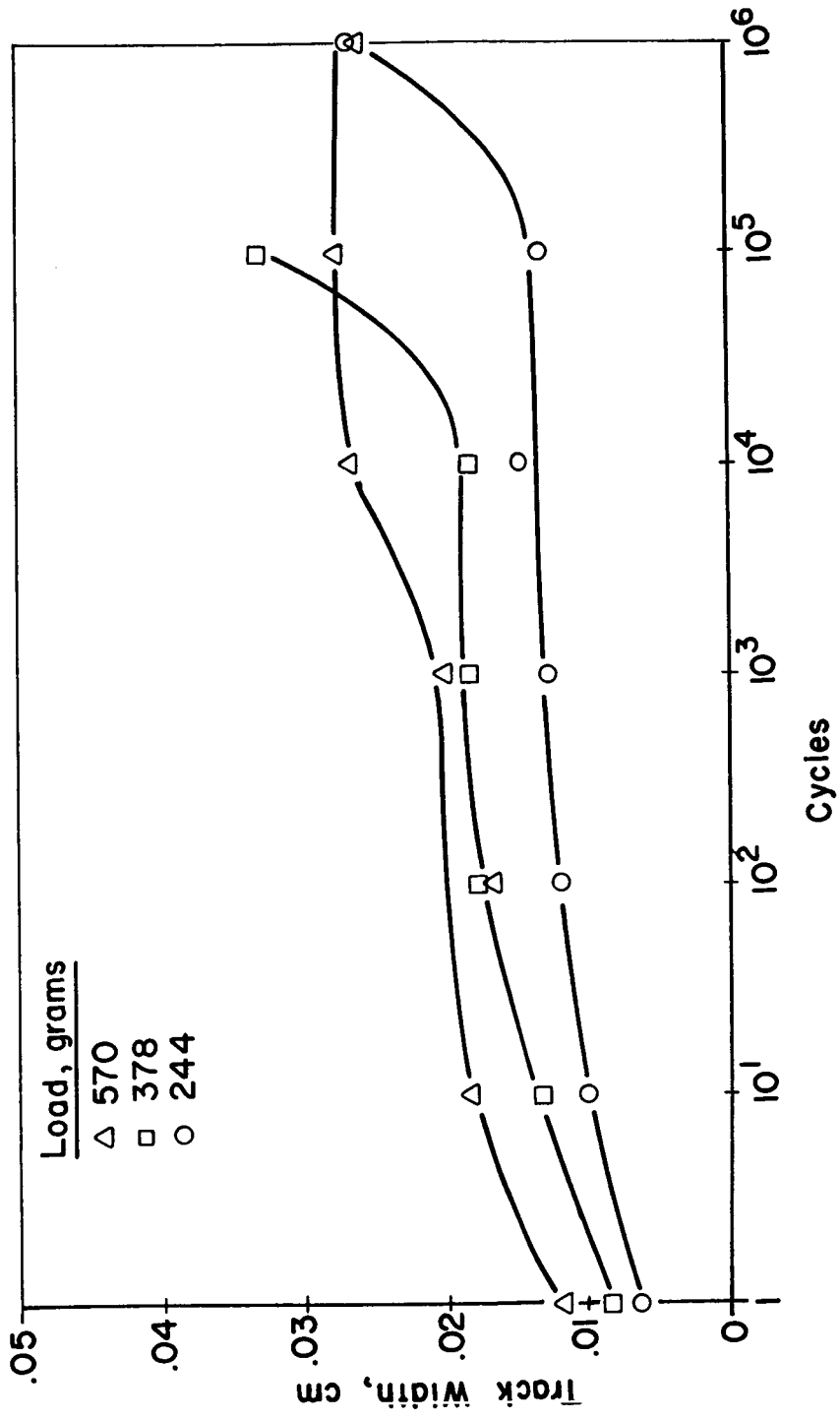

FIGURE 9. VARIATION OF TRACK WIDTH WITH NUMBER OF CYCLES FOR THE [100] BALL ROLLING DIRECTION (AFTER AMATEAU AND SPRETNAK)

ball of Haynes Stellite Alloy No. 3. The resulting track widths also are plotted in Figure 8 (dashed line) for comparison with those of previous measurements using the steel balls. It can be seen that, although the track width for the 570-gram load was smaller when the Stellite ball was used, the general shape of the curve is identical with that produced with steel balls. The increase in track width after 10^4 cycles therefore occurred even when ball wear after 10^6 cycles was reduced from an average of 100 microinches (approximately 2.5 microns) to an average of 20 microinches (approximately 0.5 micron).

Measurements of the depth of indentation in the ball paths were made by interferometry. It was found that the tracks were very shallow; the deepest was 0.7 microns (about 30 microinches), while the minimum depth was 0.18 micron (about 7 microinches). Although some wear of the MgO probably occurred, these small readings indicate that most of the track depth resulted from plastic deformation. The 0.18-micron (7-microinch) depth after one pass at 244 grams (0.54 pound) was nearly one-fourth of the 0.7-micron (30-microinch) depth after 10^6 cycles at 378 grams (0.84 pound), the deepest track. It would appear, therefore, that wear of the MgO, or changes in contact geometry resulting from plastic deformation of the MgO, did not contribute to the increase in track width after 10^4 rolling cycles.

Assuming the track-width measurements to be a rough measure of dislocation density (or extent of plastic deformation), the deformation characteristics are reminiscent of classic fatigue. The initial increase parallels the rapid initial plastic-flow phase, where dislocations are being generated and multiplied on all slip systems. The leveling out of the increase probably reflects a work hardening phase, where dislocation density has increased until dislocations begin to interact on a large scale and inhibit their free movement. The final rise in deformation might represent the unpinning phase, where dislocation pile-ups produce enough back stress to break through obstacles; this might also represent the point at which pile-up back stress becomes high enough to initiate cracks.

Track-width measurement in itself is not a completely reliable technique for measuring the extent of plastic deformation in the track prior to spalling. Actual measurement of dislocation density would be a much more reliable technique, but is quite difficult because of the very high densities present after even 100 cycles. However, since ball and track wear do not account for the variation of track width with rolling cycles, the track-width measurements do give some indication of the extent of plastic deformation. The initial rise in track width probably results from yielding of the surface under the force of the ball. After approximately 10 cycles, sufficient plastic deformation occurs to harden the track enough to support the contact stresses without further widening. The increase after 10^4 cycles probably results from mutual dislocation repulsion, which slowly but additively moves dislocation lines away from the deformed track region into areas without sufficient shear stress to normally propagate them. The spalling observed after 10^5 cycles probably is the result of fatigue cracking. Cyclic stresses in bulk specimens have been observed to cause irreversible dislocation multiplication in MgO, and continued application eventually has led to crack nucleation at the surface or at intersecting slip planes[4]. Fatigue cracks, which reach a stable size, continue to propagate under the cyclic loading and lead to gross specimen failure.

The increase in width of the tracks is not accompanied by an increase in depth of slip for the [110] rolling direction. Figure 10 shows the cross sections of two tracks after 1 and 10^6 rolling-contact cycles. The increased track width is obvious, but the depth of slip is nearly the same. This probably resulted from an interaction of dislocations on the four active {110} planes, limiting their propagation deeper into the MgO.

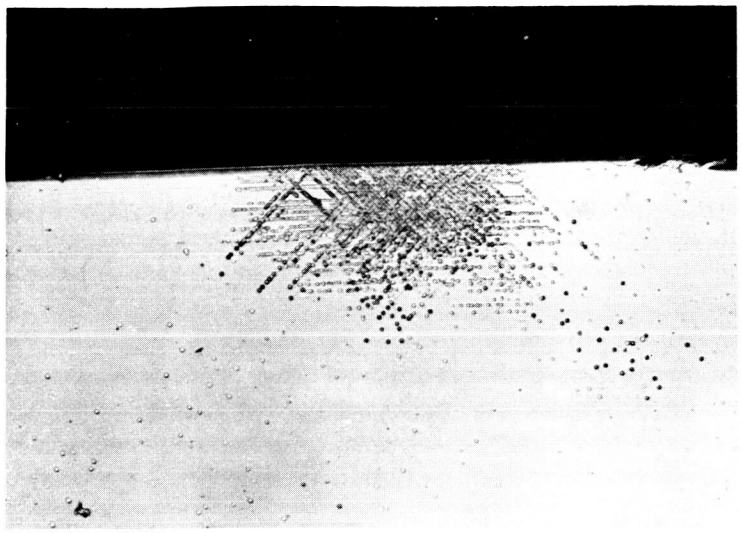

200X

(a) One rolling-contact cycle

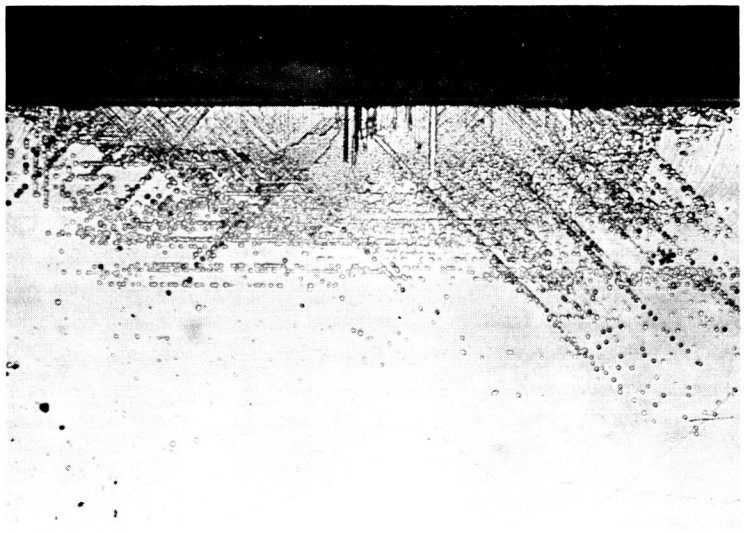

200X

(b) 10^6 rolling-contact cycles

FIGURE 10. EFFECT OF INCREASING STRESS CYCLES ON TRACK WIDTH AND DEPTH OF SLIP

244-gram load; [110] rolling direction.

One such interaction is the well-known combination of mobile dislocation on (101) and (011) planes, which intersect at 120 degrees, to form stable dislocations on {211} planes. Since the ionic bonding of MgO requires very high energy to produce slip of {211} planes, the dislocation is effectively immobilized. Subsurface deformation has been observed to be deeper at all cycle levels for the [100] rolling direction. This probably is a result of the orientation of the slip planes with respect to the rolling direction. The effects of orientation are diagramed in Figure 11. Note that in the [100] rolling direction, the loops in the (101) planes tend to move with the stress field, providing a much longer application of the contact stress on any given plane. In the [110] rolling direction, the ball moves at 45 degrees to the intersection of the slip planes with the surface, therefore applying the contact stress for a much shorter time along the slip planes. In addition, rolling in the [110] direction results in all $\{110\}_{45}$ planes being equally active in slip, increasing the chances for dislocation interaction along 120-degree intersections, as shown in Figure 11(b).

Observation of birefringence when polarized light was projected through the crystal in a polarizer microscope showed the extent of lattice distortion after rolling contact. Figure 12 is a photomicrograph under crossed nicols taken after 10^6 cycles at 378 grams (0.84 pound) contact load. Birefringence was maximum with the track placed at 45 degrees to the crossed nicols, but a rotation of 30 degrees produced the greater detail seen in Figure 12. The dark, discontinuous lines lie generally in the [100] direction, but they deviate from perfect alignment and do not intersect at 90 degrees like the primitve slip system. Birefringence in this material is caused by residual strains – either tensile or compressive. The type of strain can be distinguished by a gypsum wave plate that tints the image red in tensile or neutral regions and blue in compressive regions. When the track was viewed with alignment for maximum birefringence, the entire track appeared blue, indicating extensive residual compressive stress. When viewed in the position shown in Figure 12, the areas appearing light in Figure 12 were blue, while those appearing dark were red. The dark lines were, therefore, areas of residual tensile stress in a general track region of compressive stresses. They probably are similar to subgrain boundaries in that they separate areas of slightly different crystal orientation. Viewed on edge, the region of subsurface plastic deformation also had residual compressive stresses over the entire area of dislocation etch pits. Birefringence effects changed with increasing stress cycles. Application of a few stresses produced very little reaction to polarized light in the stressed regions. Birefringence increased with greater numbers of stress cycles, but the dark lines shown in Figure 12 were not present until after 10^5 to 10^6 cycles. This is also the range where spalling occurred. Thus, the formation of the areas similar to subgrains may be a prerequisite for spalling.

Since the MgO crystals used in this study were of optical quality, the fatigue spalls in the tracks probably did not result from inclusions, grain boundaries, or second phases originally present in the material. Therefore, spall formation was considerably simpler than in metallic bearing materials, which always contain one or more of inclusions, grain boundaries, or second phases. It would appear that crack formation in MgO was the result of dislocation interaction on intersecting slip planes. This indicates that, at least in a model material, rolling-element fatigue does not require inclusions or foreign particles for initiation. Although a similar effect could occur in metallic bearing materials, the interactions are exceedingly complicated. Studies with transmission electron microscopy will help to establish the interactions leading to crack formation in MgO.

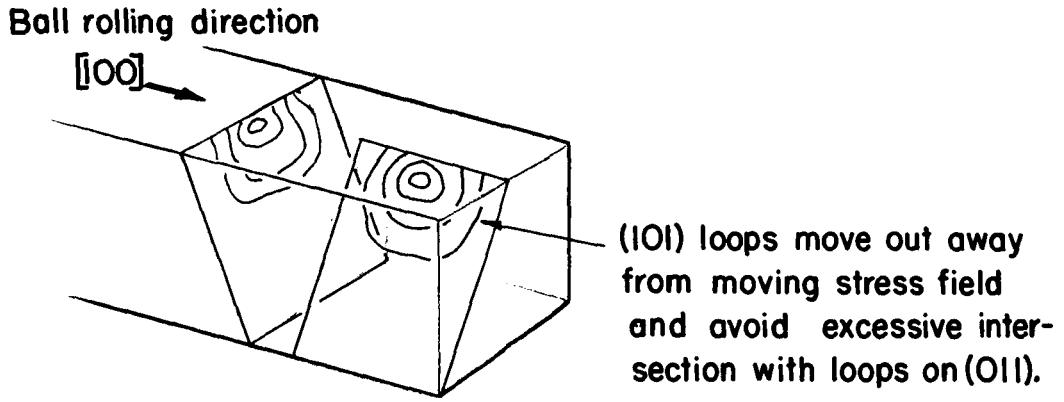

(a) Dislocation loop propagation during [100] ball rolling

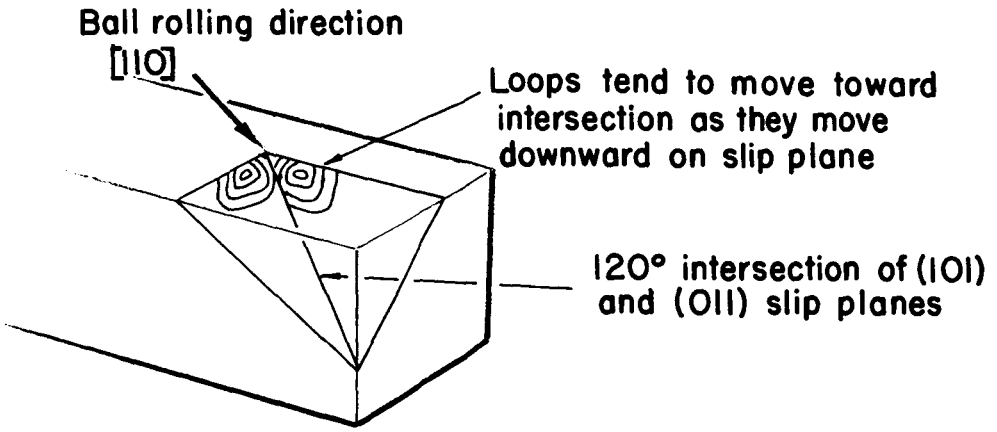

(b) Dislocation loop propagation during [110] ball rolling

FIGURE 11. EXPECTED ORIENTATION EFFECTS IN DISLOCATION LOOP INTERSECTIONS ON 120-DEGREE INTERSECTING PLANES

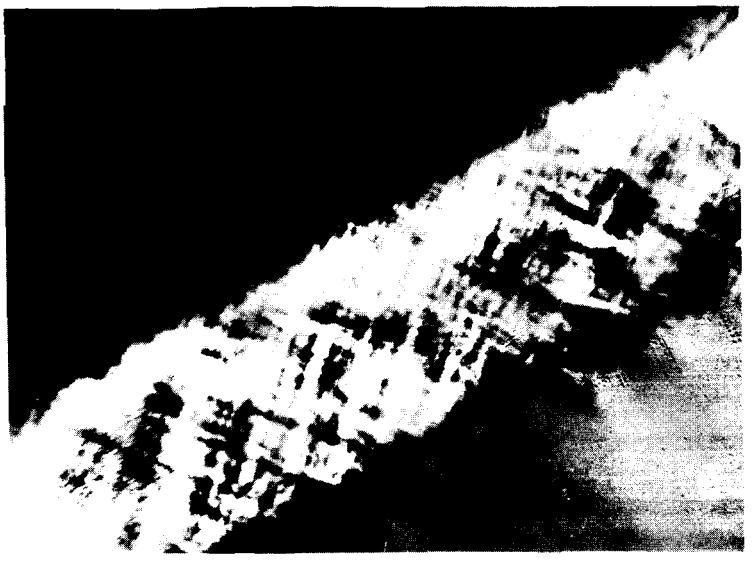

FIGURE 12. BIREFRINGENCE AFTER 10^6 STRESS CYCLES WITH 378-GRAM LOAD AND [110] ROLLING DIRECTION

Lubrication Studies

As part of the effort to reduce ball wear in the fatigue experiments, the specimens were flooded with lubricants during rolling contact. A marked change in slip characteristics occurred after relatively few rolling cycles, producing very unusual results.

Experimental Method

The rolling velocity and specimen preparation were identical with those of the previous dry rolling-element-bearing fatigue experiments, except that a 570-gram (1.26-pound) ball load was used exclusively. The fluids used included 10-cs and 250-cs pure silicone oil, 10-cs white additive-free mineral oil, kerosene, kerosene containing 3 percent stearic acid, alcohol, and water. For comparison purposes, identical experiments were performed on the same specimen under dry and flooded conditions. The specimens were then cleaved, etched, and examined in the usual manner.

Results and Discussion

Specimens were submitted to rolling contact in the [100] rolling direction while lubricated to determine the effect on slip characteristics. Silicone oil (10 cs) was used initially. Tracks with 1, 10, 100, and 1000 cycles first were made on a given specimen, followed by a similar set of four tracks with the specimen flooded with oil. Comparison of the tracks with and without oil showed no difference after one rolling cycle. All slip occurred on the $\{110\}_{45}$ planes, as in dry rolling. However, after 10 cycles with oil, slip on $\{110\}_{90}$ planes became evident, an unusual occurrence because the resolved shear stresses on this set of easy glide planes have been assumed small compared with the maximum shear stresses at 45 degrees to the surface. After 100 cycles, slip on the $\{110\}_{90}$ planes became very prominent, and numerous small pits appeared along the track.

After 1000 cycles, the effect was even more pronounced. Figure 13 shows two tracks on the same specimen after 1000 cycles with and without the 10-cs silicone oil. The track with lubricant present is obviously wider, and slip on the $\{110\}_{90}$ planes is very evident (rows of etch pits intersecting the track at 45 degrees). Cross sections of the tracks were similar, showing the depth of slip on the $\{110\}_{90}$ planes to be very small. Measurements of the actual depth of slip, made by polishing layers off the surface with phosphoric acid, showed that most of the $\{110\}_{90}$ slip was confined to 10 percent of the total deformed depth and all of it to 25 percent of the deformed depth.

The reason for the dramatic change in slip characteristics was not immediately obvious. Possible effects considered included surface chemical activity, alteration in tractive characteristics by fluid dynamics, change in surface energy by adsorption, and pinning of screw components by selective adsorption of polar molecules on dislocation cores intersecting the surface.

Lubrication with higher viscosity 350-cs silicone oil produced the same effect as lubrication with 10-cs silicone oil. Use of the high-viscosity oil did appear to reduce the severity of surface damage, however. After approximately 2000 cycles with 10-cs oil lubrication, the track was completely spalled. Although identical spalling and $\{110\}_{90}$ slip occurred with 350-cs oil lubrication after 1000 cycles, the track was not completely spalled after 146,000 cycles. Thus, although the higher viscosity apparently did delay the onset of severe damage, it did not change the predominance of $\{110\}_{90}$ slip planes. A number of experiments were carried out to investigate the influence of the above factors on the unexpected behavior with liquid lubricant. The same effect was produced when an additive-free super-refined mineral oil was used. This lubricant is relatively inert and was not expected to enter into any surface chemical reaction with MgO.

It was conjectured that perhaps selective adsorption at sites where screw dislocations intersect the surface might inhibit cross slip and produce early strain hardening. This theory was tested by using a 3 percent solution of stearic acid in kerosene as a lubricant. Slip on $\{110\}_{90}$ planes and early spalling was again produced when either pure kerosene or kerosene with stearic acid was used. The extent of spalling was reduced when the stearic acid was used. No difference in the predominance of $\{110\}_{90}$ slip was observed.

It is known that MgO reacts with water to form a hydride. Moisture in the air is sufficient to turn the surface of exposed MgO milky in a few days. It was conjectured that water in solution in the fluids used as lubricants was reacting with the MgO surface and the alteration in surface structure was leading to early spalling. An experiment was performed using water as a lubricant. Surprisingly, the runs with water produced results similar to dry rolling experiments. In addition, it was found that alcohol produced the same result as water.

The influence of orientation on the change in slip mode was determined by rolling the ball in the [110] direction with silicone oil lubrication. Slip on $\{110\}_{90}$ planes was promoted, as it was in experiments in the [100] rolling direction. The number of cycles to promote spalling was larger, however. Approximately 10^4 cycles were required for formation of spalls, compared with 10^3 cycles for the [100] rolling direction. The appearance of the spalls was similar for both rolling directions.

Since the rolling velocity used was very low and the contact area small, it seems unlikely that a hydrodynamic film was produced between the ball and MgO flat. This was confirmed further by the lack of a viscosity effect seen when viscosities ranging from

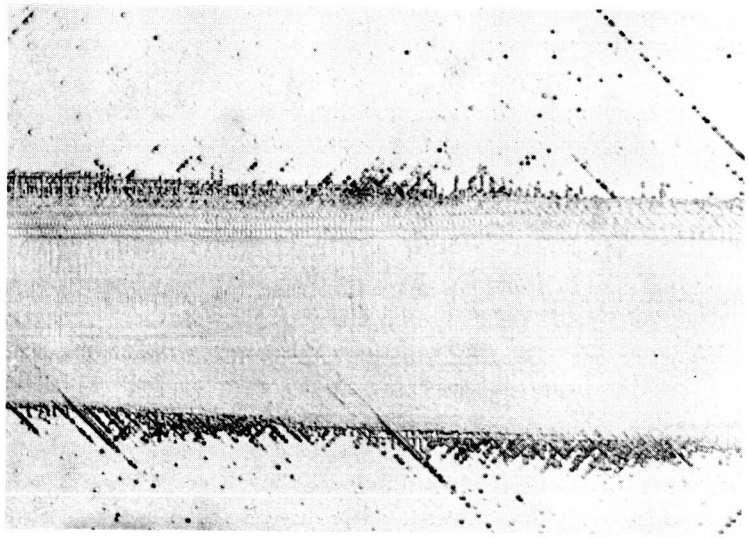

(a) Dry

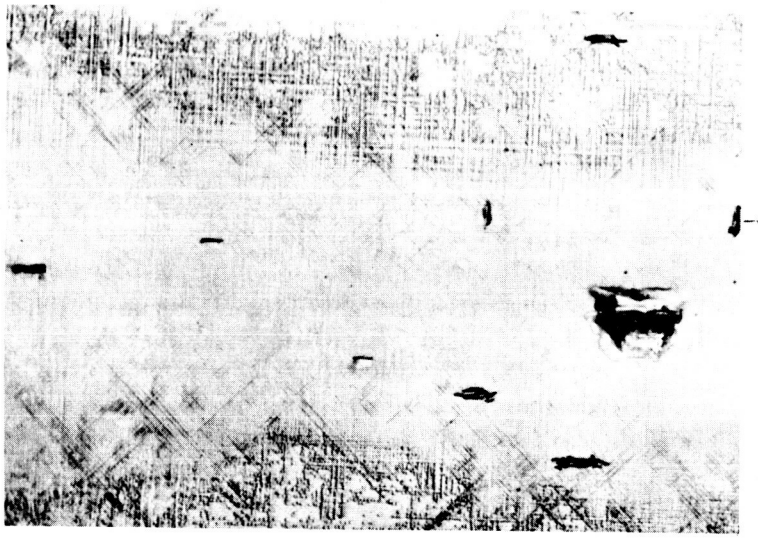

200X

(b) Lubricated with 10-cs silicone oil

FIGURE 13. CHANGE OF SLIP CHARACTERISTICS RESULTING FROM PRESENCE OF LUBRICANT IN ROLLING CONTACT

1000 cycles with 570-gram load, [100] rolling direction.

kerosene to 350-cs silicone oil produced similar changes in slip modes. The contact stresses also would be significantly changed if traction were lost, causing high tangential friction forces. Experiments using lubricants with pure ball sliding or with a one-to-one slide-roll ratio were performed to determine the influence of sliding on change of slip mode. After only 10 cycles, the ball and track damage was quite severe through heavy scoring, showing that high friction was present, with little fluid-film lubrication. Slip on $\{110\}_{90}$ planes was extensive, but it was not likely that the mechanism was the same that caused the $\{110\}_{90}$ slip in lubricated rolling.

Surface chemical interactions between the lubricants and MgO appear most likely as the mechanism. Although the silicone and light mineral oil are known to be very inert and no reaction between them and MgO is known to exist, it may be possible that a reaction is promoted by the combination of high contact stresses and the presence of hydrates caused by reactions between the MgO surface and water prior to testing. To produce the slip observed on the $\{110\}_{90}$ planes, the reaction would require promotion of movement of edge dislocations, which intersect the surface on $\{110\}_{90}$ planes, or inhibition of the movement of screw dislocations, which intersect the surface on $\{110\}_{45}$ planes (see Figure 2). It is more likely that an inhibition of movement of screw dislocations would produce the observed results. Since dislocation loops can multiply by cross slip of screw components, thereby spreading slip from single slip planes to nearby parallel planes, an increase in total plastic strain would result as rolling stress cycles are increased. However, if screw components intersecting the surface are pinned by surface reactions, stress cycles will build up a concentration of dislocations on original slip planes and build up stress concentrations at slip-plane intersections. The resulting stress concentrations could then initiate dislocations and slip on a new set of slip planes, $\{110\}_{90}$.

Limited experiments were made with compression specimens to determine the influence of lubricants on bulk mechanical properties. Yield characteristics in single, dislocation-free crystals are surface sensitive, since dislocations originate and multiply at the surface. Compression tests of single-crystal specimens, both lubricated and dry, were performed to see if changes in yield characteristics could be detected. No change in yield strengths, flow properties, or elongation was observed as a result of lubricants on the crystal surfaces. Although these results were negative, it may be possible that the bulk interior properties were overwhelming any strength alterations resulting from changes in slip mode caused by surface reactions between the lubricants and MgO.

The surface reaction between water and MgO may have an important bearing on the observed effects. Let us suppose that reaction with water molecules hardens the surface of MgO. During rolling contact, Heathcote slip in the contact area will produce tangential forces in the surface. These forces are probably not sufficient to operate $\{110\}_{90}$ slip systems at the hardened surface. When oil is used, however, it can shield the surface from water vapor, and as the hardened surface is removed by attrition, the weaker substrate is exposed and surface sources begin to operate under the tangential forces. This might explain the anomalous behavior when water was used as a lubricant.

The spalling observed after only 1000 rolling cycles probably resulted from dislocation interactions on the intersecting $\{110\}_{90}$ planes. The effect of slip plane orientation on dislocation pile-up is shown in Figure 14. Note that only $\{110\}_{90}$ planes form orthogonal intersections at the crystal surface. At these intersections, edge components interact and pile up. These pile-ups can only be relieved by climb, which is difficult in ionic solids. Intersection of $\{110\}_{45}$ planes produces interaction of screw components at the surface. As noted before, the $\{110\}_{45}$ interactions can be relieved by cross slip of screw

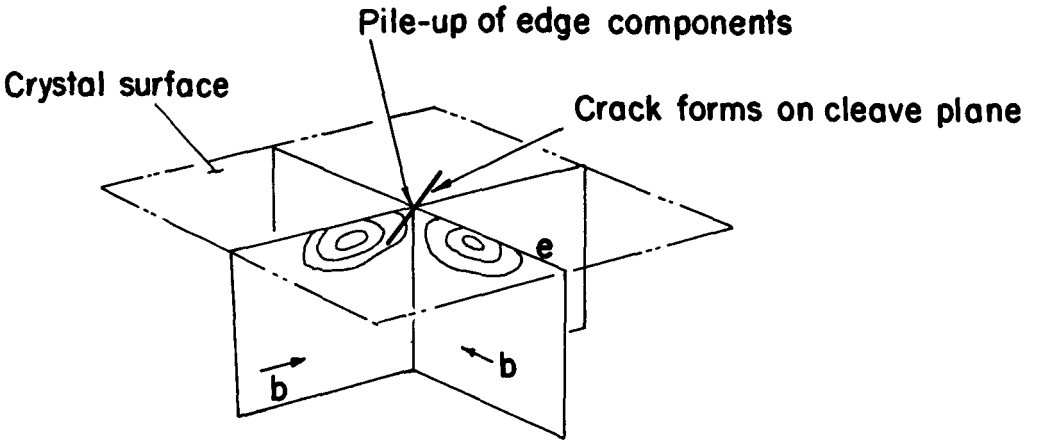

(a) Dislocation loops on intersecting $\{110\}_{90°}$ planes. Edge components at surface pile up at intersection. Pile up can be relieved only by climb or reversal of stress.

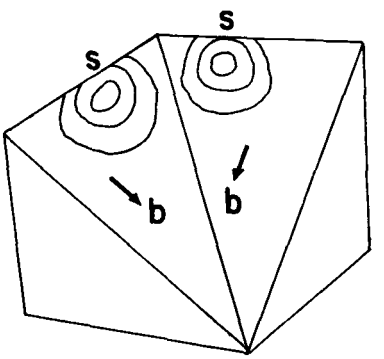

(b) Dislocation loops on intersecting $\{110\}_{45°}$ planes. Mixed screw and edge configuration at intersection allowing some cross-slip and dislocation reactions to form new dislocations.

FIGURE 14. INTERACTION OF DISLOCATION LOOPS ON INTERSECTING PLANES, SHOWING THE EFFECT OF PLANE ORIENTATION ON POSSIBLE PILE-UP AND CRACK FORMATION

components to fresh $\{110\}_{45}$ slip planes. Subsurface intersections of loops where screw components cut edge components can result in jogs and dipoles. Washburn, et al.[5], have demonstrated that cracks will nucleate at the intersection of slip bands on orthogonal planes. In a more detailed study, Chou and Whitmore[6] describe three possibilities for crack formation: (1) single pile-up arrested by a slip band and initiation of {110}-type cracks, (2) double pile-up on two orthogonal {110} slip planes, forming {100}-type cleavage cracks (the type seen in Figure 13), and (3) double pile-up on two {110} slip planes intersecting at 120 degrees, forming {110}-type cracks. Both of the first two possibilities exist for the $\{110\}_{90}$ slip planes, and both types of cracks have been observed around the spalls formed in tracks made with lubricated rolling. Since many of the spalls have edges that follow crystallographic directions, it is unlikely that a true fatigue process was responsible. Most of the spalls that formed after 10^5 cycles without lubrication did not follow crystallographic directions and probably represent a true fatigue cracking.

Since the lubricants and MgO used in this study were relatively inert compared with actual bearing materials, it is interesting to speculate on what effect surface reactions may have on the life of actual bearings. If surface reactions exist that influence the predominant slip mode, it may be possible to greatly reduce or extend bearing life by controlling these reactions. Dislocation interactions that nucleate stable cracks also occur at intersecting slip systems in metals. If slip were inhibited on systems that form cracks in orientations most likely to propagate, perhaps a significant extension of bearing life could be realized. In addition, the early spalling observed has some aspects of fretting wear. The interaction of surface-active lubricants and dislocations intersecting the surfaces of crystals may have a profound influence on the onset of fretting damage. It is possible, then, that fluid species could influence fretting rates and that presumed "benign" fluids may actually promote fretting.

Transmission Electron Microscopy

Transmission electron microscopy provides information on dislocations that cannot be obtained by etch-pit techniques. Dislocation lines and their interactions can be viewed directly, and the technique is not as limited by high dislocation densities as is the etch-pit technique. Thus, instead of seeing slip planes outlined by a multitude of pits that indicate dislocation terminals, actual distributions of dislocation lines, dipoles, loops, and tangles can be seen by transmission electron microscopy.

Experimental Method

The preparation of thin films suitable for examination of the ball track required the development of a suitable technique. Tracks of 100 cycles were placed at close intervals to allow their edges to nearly touch, thereby increasing the chances of producing a thin film in a track region. Tracks were made with and without a light mineral oil lubricant.

Specimens for thinning, measuring 0.1 x 0.1 x 0.02 inch (0.25 x 0.25 x 0.05 cm), were cleaved from the bulk specimen and painted on the top (track side) and edges with an acid-resisting paint. A jet of phosphoric acid at 230 F impinged on the unpainted side to thin the specimen. Thinning was continued until an area was produced that was 10 to 30 microns (0.0004 to 0.0012 inch) thick. Thickness measurements were made by focusing on the top and bottom surfaces of the specimen with a depth-of-focus measuring microscope. When the required thickness was obtained, the acid-resisting paint was removed

from the specimen with acetone. Thinning was further continued in a beaker of hot phosphoric acid until an area exhibiting interference fringes appeared when the specimen was examined with a light microscope. The thinning process was very carefully monitored to prevent forming a hole. When interference fringes appeared, the specimen was further thinned in a 2:1 solution of phosphoric acid and alcohol at room temperature. This solution greatly reduced the rate of polishing and permitted further thinning until first-order interference fringes appeared at the thinnest region when examined by light microscopy. These regions were found to be sufficiently thin for direct examination by transmission electron microscopy.

The thin films were examined on a tilting stage of the electron microscope so they could be oriented to produce maximum contrast of dislocation images. The film surfaces were coated with carbon by vapor deposition to drain off charge buildup expected for a nonconducting material such as MgO. Charge buildup will cause flutter of the electron beam and result in poor resolution of dislocation images.

Results and Discussion

The initial electron microscopy was directed at comparing dislocation configurations in the ball paths resulting from dry rolling contact with those from mineral oil-lubricated rolling contact. Single-crystal specimens were subjected to 100 rolling cycles, 570-gram (1.26-pound) load, with and without lubrication. Thin-film transmission specimens were made in the ball paths close to the contact surface. Typical electron micrographs are shown in Figure 15. Figure 15(a) is shown at a lower magnification (6500X) than Figure 15(b) (16,200X), because $\{110\}_{90}$ slip systems in Figure 15(a) do not show up as well at the higher magnification. The heavy lines crossing each other at right angles in Figure 15(a) are the $\{110\}_{90}$ slip planes observed in the etch-pit studies of the lubricated rolling-contact experiments. The specimen is oriented so that the (100) surface is in the plane of the micrograph and the [100] direction (rolling direction in this case) is shown by the arrow. The individual dislocations in the $\{110\}_{90}$ slip planes cannot be resolved, because the planes containing them are viewed on edge. The large concentration of $\{110\}_{90}$ slip planes typical in Figure 15(a) was not seen in the specimen from the dry rolling-contact experiment and confirmed the conclusion from the etch-pit studies that lubricated rolling contact activates $\{110\}_{90}$ slip at the surface of the MgO crystal. Since crack initiation was expected at $\{110\}_{90}$ intersections, the field of intersections in the specimen shown in Figure 15(a) was searched for embryo cracks. No evidence of them was found. More such studies will be required before any conclusions can be drawn concerning the role of $\{110\}_{90}$ dislocation interactions in cleavage-type cracks shown in Figure 13(b).

One feature that is quite noticeable in Figure 15(a) is the concentration of dislocations in bands on both $\{110\}_{45}$ and $\{110\}_{90}$ planes. This was found for both dry and lubricated rolling contact. This behavior, in which slip is concentrated in zones separated by unslipped material, has been observed for MgO crystals subjected to bending-fatigue conditions.[7]

The photomicrograph in Figure 15(b) shows details of individual dislocations on $\{110\}_{45}$ planes after 100 cycles of dry rolling contact. Even after 100 cycles, the dislocation density is very high. (The black spots are artifacts and should be disregarded.) The dislocations shown are on planes oriented at 45 degrees to the plane of the micrograph, and therefore individual dislocations can be seen. In general, the dislocation lines

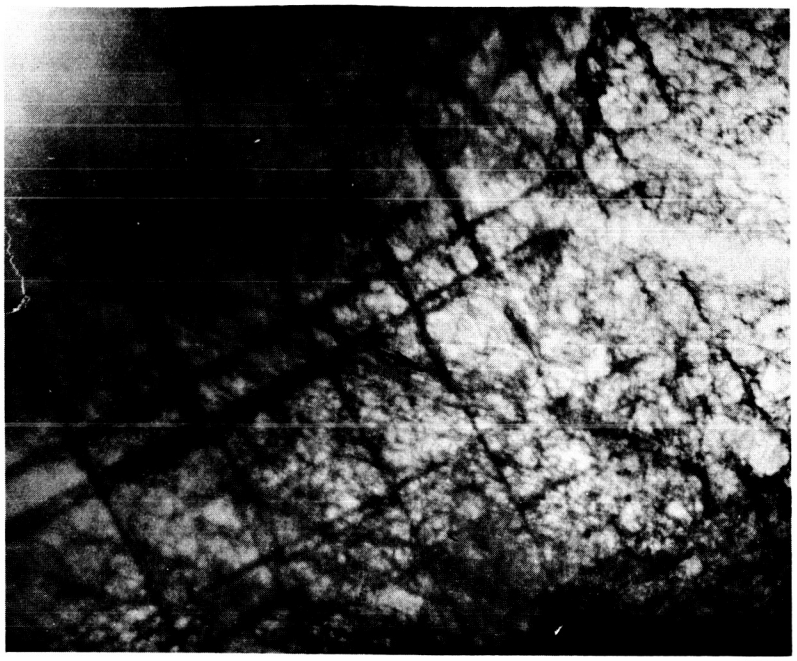

6500X

(a) With lubrication

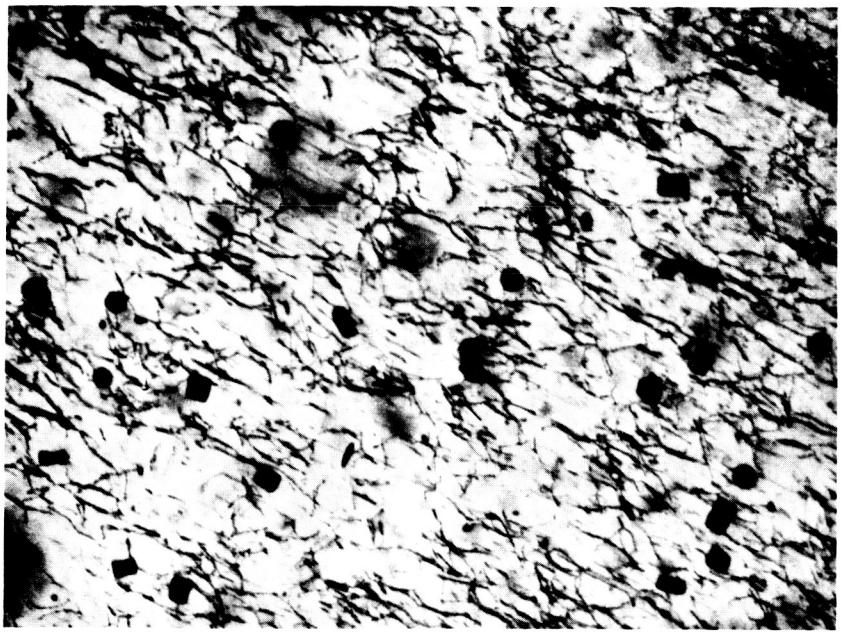

16,200X

(b) Dry rolling

FIGURE 15. TRANSMISSION ELECTRON MICROGRAPHS OF DRY AND LUBRICATED TRACK REGIONS AFTER 100 CYCLES WITH 570-GRAM LOAD

in Figure 15(b) are lined up in the [100] direction. The dislocation lines are broken up with many angular jogs resulting from the intersection of dislocations on other cutting slip planes. The jogged and fragmented nature of the dislocations in Figure 15(b) is typical of a type of work hardening. It indicates that the interaction and pinning of dislocations is well under way after 100 cycles of rolling contact.

These initial studies with transmission electron microscopy have indicated that, as a supplement to etch-pit analysis, it should provide valuable additional information for an eventual three-dimensional reconstruction of dislocation distributions as they are influenced by rolling-contact stress. Typical dislocation arrays for the various stages of rolling-element deformation, from the first cycle to the second rise in the curve of track-width versus cycles, and spalling eventually can be determined in this way.

SUMMARY OF RESULTS

The dislocation distribution in single-crystal MgO as the result of rolling-contact stress has been studied. Repeated stressing of single crystals until spalling has been carried out. The effects of stress cycles, rolling velocity, orientation, and liquid lubrication on dislocation arrays has been determined. The following results and conclusions were obtained:

(1) Spalling similar to that found in bearing and gear surfaces could be produced without the presence of inclusions, carbides, grain boundaries, or other discontinuities. Spalling was assumed to be the result of subsurface structural damage by dislocation interaction.

(2) Stressing by rolling contact produces a characteristic dislocation pattern because of the special condition of a small, moving stress field interacting with moving dislocations.

(3) The depth of plastic strain, and hence the amount of plastic relief to the stressed portion of the crystal, is influenced by ball velocity. It is expected that the frequency of dislocation interaction would decrease as a function of load and rolling velocity and the sensitivity of this effect would decrease with decreasing grain size.

(4) Plastic deformation from repeated rolling contact builds up in three phases: (1) rapid increase in deformation extent, (2) slow-deformation work hardening, and (3) increase in deformation. Spalling occurs during the third phase.

(5) The presence of liquid lubrication induces dislocation propagation on planes not active during dry rolling contact. Surface interaction of slip planes activated by lubricants results in the generation of cleavage cracks and very early shallow spalling. The lubricant either pins screw dislocations at the surface (by adsorption at dislocation sites) and causes slip on other, more damaging slip systems, or it prevents formation of a protective layer (reaction with atmosphere that inhibits surface generation of damaging slip systems).

REFERENCES

(1) Amateau, M. F., and Spretnak, J. W., "Plastic Deformation of Magnesium Oxide Crystals Subjected to Rolling Contact Stresses", Journal of Applied Physics, Vol. 34, No. 8, pp. 2340-2345 (August, 1963).

(2) Gilman, J. J., Knudsen, C., and Walsh, W. P., "Cleavage Cracks and Dislocations in LiF Crystals", Journal of Applied Physics, Vol. 29, No. 4, pp. 601-607 (April, 1958).

(3) Johnston, W. G., "Deformation Mechanisms of Refractory Materials", Progress Report No. 2, Contract AF 33(616)-7942 (November, 1962).

(4) Cornet, I., and Gorum, A. E., "The Observation of Fatigue Processes in MgO Single Crystals", Trans. Met. Soc. AIME, Vol. 21B, pp. 480-485 (June, 1960).

(5) Washburn, J., Gorum, A. E., and Parker, E. R., "Cause of Cleavage Fractures in Ductile Materials", Trans. Met. Soc. AIME, Vol. 215, pp. 230-237 (1959).

(6) Chou, Y. T., and Whitmore, R. W., "Single and Double Pile-Up of Dislocations in MgO Crystals", Journal of Applied Physics, Vol. 32, No. 10, pp. 1920-1926 (October, 1961).

(7) Alden, T. H., "The Strain Hardening of Magnesium Oxide Single Crystals", Trans. Met. Soc. AIME, Vol. 227, pp. 1103-1108 (October, 1963).

DEFINITIONS

Burger's vector – the closure failure of an atom-to-atom loop around a dislocation; such a loop taken in a perfect crystal would close upon itself.

Cross slip – motion of a dislocation on a plane inclined to that on which it was moving previously; limited to nondissociated screw dislocations.

Dislocation – line defect separating slipped from nonslipped regions of a crystal.

Dislocation density – length of dislocation line per unit volume of material; usually measured as the number of dislocations intersecting a unit area.

Dislocation dipole – pairs of parallel mixed or edge dislocations with mutual distance comparable to the basic lattice dimension.

Dislocation jog – a step in the dislocation in the direction of the dislocation line.

Dislocation loop – a dislocation line terminating on itself entirely within the crystal.

Dislocation tangle – interaction of dislocations on various slip planes.

Edge dislocation – dislocation characterized by the Burger's vector being normal to the dislocation line.

Etch pit – pit formed at the intersection of a dislocation line with a surface as a result of etching.

Fcc lattice – spatial distribution of atoms in which atoms occupy the corners of the cube and the centers of all six faces; see Figure 1(a).

Miller indices – method of uniquely describing crystallographic planes and directions.

Mixed dislocation – dislocation consisting of both edge and screw components.

Screw dislocation – dislocation characterized by the Burger's vector being parallel to the dislocation line.

Sessile dislocation – a dislocation line that is not free to move by glide, but can move by climb.

KFD:WAG/jb

DISTRIBUTION LIST

NASA Headquarters
Washington, D. C. 20546
Attention: N. F. Rekos (RAP)
M. Comberiate

NASA-Lewis Research Center
21000 Brookpark Road
Cleveland, Ohio 44135
Attention: John H. DeFord, M.S. 60-5
Technology Utilization Office, M.S. 3-19
P. T. Hacker, M.S. 5-3
I. I. Pinkel, M.S. 5-3
J. Howard Childs, M.S. 60-4 (2 copies)
D. Townsend, M.S. 60-4 (4 copies)
L. Macioce, M.S. 60-4
E. E. Bisson, M.S. 5-3
R. L. Johnson, M.S. 23-2
W. J. Anderson, M.S. 23-2
E. V. Zaretsky, M.S. 6-1 (12 copies)
Reports Control Office, M.S. 5-5

FAA Headquarters
800 Independence Avenue, S.W.
Washington, D. C. 20553
Attention: F. B. Howard/SS-120
Brig. General J. C. Maxwell

Air Force Materials Laboratory
Wright-Patterson AFB, Ohio 45433
Attention: MANL
R. Adamczak & F. Harsacky
MAMD
Walter Trapp

NASA-Langley Research Center
Langley Station
Hampton, Virginia 23365
Attention: Mark R. Nichols

United Aircraft Corporation
Pratt & Whitney Aircraft Division
East Hartford, Connecticut 06108
Attention: R. P. Schevchenko
P. Brown

General Electric Company
Gas Turbine Division
Evendale, Ohio 45215
Attention: B. Venable
E. N. Bamberger

California Research Corporation
Richmond, California 94802
Attention: Douglas Godfrey

Dow Chemical Company
Abbott Road Buildings
Midland, Michigan 48640
Attention: Dr. R. Gunderson

Crucible Steel Company of America
The Oliver Building
Mellon Square
Pittsburgh, Pennsylvania 15222

Dow Corning Corporation
Midland, Michigan 48640
Attention: R. W. Awe & H. M. Schiefer

Allegheny Ludlum Steel Corporation
Oliver Building
Pittsburgh, Pennsylvania 15222

Mechanical Technology, Incorporated
Latham, New York 14603
Attention: B. Sternlicht

Director
Government Research Laboratory
Esso Research & Engineering Company
P.O. Box 8
Linden, New Jersey 07036

Industrial Tectonics, Inc.
Research & Development Division
18301 Santa Fe Avenue
Compton, California 90220
Attention: Heinz Hanau

Monsanto Research Corporation
Everett Station
Boston, Massachusetts 02109
Attention: Dr. John O. Smith

Pennsylvania State University
Department of Chemical Engineering
University Park, Pennsylvania 16801
Attention: Dr. E. E. Klause

Fafnir Bearing Company
37 Booth Street
New Britain, Connecticut 06051
Attention: H. B. Van Dorn

General Electric Company
General Engineering Laboratory
Schenectady, New York 12305

DISTRIBUTION LIST (Continued)

Borg-Warner Corporation
Roy C. Ingersoll Research Center
Wolf and Algonquin Roads
Des Plaines, Illinois 60016

General Motors Corporation
New Departure Division
Bristol, Connecticut 06010
Attention: W. O'Rourke

Franklin Institute Labs
20th and Parkway
Philadelphia, Pennsylvania 19133
Attention: Otto Decker

Westinghouse Electric Corporation
Research Laboratories
Beulah Road, Churchill Borough
Pittsburgh, Pennsylvania 15235
Attention: John Boyd

Midwest Research Institute
425 Volker Boulevard
Kansas City, Missouri 64110
Attention: V. Hopkins & A. D. St. John

Socony Mobil Oil Company
Research Department
Paulsboro Laboratory
Paulsboro, New Jersey 08066
Attention: Ed. Oberright

The Marlin-Rockwell Corporation
Jamestown, New York 14701
Attention: Arthur S. Irwin

Southwest Research Institute
San Antonio, Texas 78205
Attention: P. M. Ku

IIT Research Institute
West 35th Street
Chicago, Illinois 60616
Attention: Warren Jamison

NASA-Lewis Research Center
21000 Brookpark Road
Cleveland, Ohio 44135
Attention: Library

Sinclair Research, Incorporated
400 E. Sibley Boulevard
Harvey, Illinois 60426
Attention: M. R. Fairlie
Director of Products Division

NASA-Scientific and Technical Information Facility
Box 5700
College Park, Maryland 20740
Attention: NASA Representative (6 copies)

AiResearch Manufacturing Company
Dept. 93-3
9851 Sepulveda Boulevard
Los Angeles, California 90009
Attention: Hans. J. Poulsen

Department of the Army
U. S. Army Aviation Material Labs.
Fort Eustis, Virginia 23604
Attention: J. W. White
Propulsion Division

SKF Industries, Inc.
Engineering & Research Center
1100 First Avenue
King of Prussia, Pennsylvania 19104
Attention: L. B. Sibley
T. Tallian

Nyatt Division
New Departure Bearing Company
Sandusky, Ohio 44870
Attention: B. Ruley

Timkin Roller Bearing Company
Canton, Ohio 44701
Attention: Dr. W. Littmann

Caterpillar Tractor
Peoria, Illinois 61601
Attention: B. Kelley

General Motors Research Laboratory
Warren, Michigan 48089
Attention: Nils L. Buench

Department of the Navy
Naval Ship Research
Development Center
Annapolis, Maryland 21402
Attention: Paul Schatzberg